2008-01-2966

Comparison of the Performance of 7-Post and 8-Post Dynamic Shaker Rigs for Vehicle Dynamics Studies

Steve C. Southward and Christopher M. Boggs
Virginia Tech

ABSTRACT

This paper documents a simple theoretical analysis and an experimental performance comparison of the advantages of an 8-post shaker rig relative to a conventional 7-post shaker rig. A simple static model describing the chassis roll and warp characteristics is first presented to illustrate the differences between 7-post and 8-post configurations, and the conditions where an additional aeroloader provides an advantage. Using a late model NASCAR Sprint Cup car, a series of experimental tests were conducted with the 8-post shaker rig at the Virginia Institute for Performance Engineering and Research (VIPER) facility in both 7-post and 8-post configurations. Experimental results confirm the hypothesis that an 8-post configuration is able to more accurately reproduce target motions of the chassis and suspension when those motions include a chassis warp condition.

INTRODUCTION

Successful race teams look for every possible advantage over their competition to reduce lap times and win the race. While track testing is ultimately the most valid testing method available, the amount of time and resources it takes to find the ideal setup alone is prohibitive. The most common alternative for evaluating vehicle behavior is a 7-post shaker rig. Compared to track testing, rig testing is more repeatable, costs less, and can be conducted around the clock [1, 2, 3, 4].

While shaker rig testing is an attractive and common option, race teams must consider the potential problems that can have a negative impact on the fidelity of the test results. A conventional 7-post shaker rig applies aeroloader forces to the chassis at only three points in order to simulate the aerodynamic and inertial loads that excite the chassis on the track. Assuming that the chassis is rigid, three aeroloaders are sufficient to control chassis heave, pitch, and roll motions. In open-wheel racing, where 7-post rig testing originated, the chassis is much stiffer than the suspension, and this assumption is justified. Although it is often desirable for the chassis to be relatively rigid in torsion [5], this is not usually the case. When this condition is violated, and the chassis torsional stiffness is closer to the suspension stiffness, the ability of only three aeroloaders to accurately reproduce chassis and suspension motions on a 7-post rig is degraded. The use of four aeroloaders, as in an 8-post shaker rig, provides the additional degree of freedom that is required to control the rigid body modes, i.e. pitch, roll, and heave, as well as the warp mode of the chassis.

STATIC WARP MODEL

To illustrate the theoretical differences between 7-post and 8-post shaker rigs, we first present a simple static model for chassis roll and warp. This model is very similar to the model developed by Deakin et. al. [6]. The aeroloaders are designed to apply forces that represent the aerodynamic and inertial forces that are distributed across the chassis on the racetrack.

The forces generated by aeroloaders and applied to the chassis on either a 7-post or an 8-post shaker rig may be decomposed into dynamic modes as a heave force, a pitch moment, a roll moment, and a warping moment. For this analysis, we are not interested in the heave

force or pitch moment, therefore, the static roll and warp behavior may be approximated by a simple torsional spring model, as shown in Figure 1. The reason the roll and warp modes are of interest is because they are intimately coupled on a 7-post rig. In fact, a 7-post rig must induce a roll condition in order to create warp, whereas an 8-post rig can create a pure warp without any roll, or a pure roll without any warp.

The front and rear net roll stiffness, created from springs, antirollbars, tires, and suspension geometry, are represented by two torsional springs, k_F and k_R respectively. The angular deflection of these torsional springs corresponds to the front and rear chassis roll angles, θ_F and θ_R respectively, while the moment in the springs corresponds to the front and rear rolling moments.

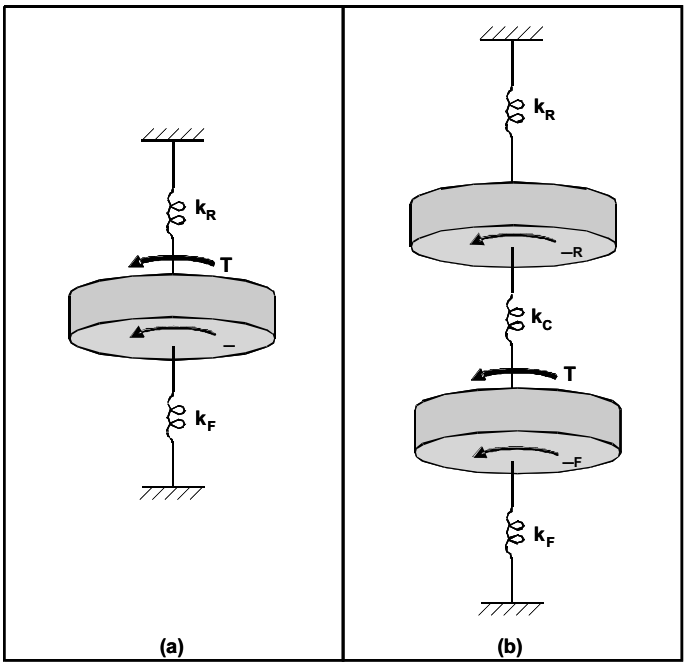

Figure 1. Static Model: (a) Rigid chassis, (b) Compliant chassis

The chassis may either be modeled as rigid or compliant. The rigid chassis model ($\theta = \theta_F = \theta_R$) is valid when the chassis stiffness (k_C) is high relative to the axle stiffness or when the forces applied to the chassis do not induce much chassis warp. The chassis warp is defined to be the relative twist from front to rear:

$$\theta_{warp} = \theta_F - \theta_R. \tag{1}$$

Figure 1a depicts the condition where the chassis is rigid. In this case, the front of the chassis rolls the same amount as the rear of the chassis when any roll moment is applied by the aeroloaders. If the chassis is rigid, a fourth aeroloader is redundant so three aeroloaders are sufficient to control three modes. Figure 1b depicts the compliant chassis case. When the chassis is compliant, the front and rear of the chassis have independent roll angles when a torsional moment is induced by the aeroloaders or through the suspension itself.

For a 7-post rig with static excitation from two aeroloaders in front and one aeroloader in the rear, and a compliant chassis as shown in Figure 1b, the rear of the chassis will always roll less than the front of the chassis by the relationship:

$$\frac{\theta_R}{\theta_F} = \left(\frac{1}{1 + \frac{k_R}{k_C}} \right) \tag{2}$$

A 7-post configuration must produce static roll angles and rolling moments as defined by this ratio. This relationship is plotted in Figure 2.

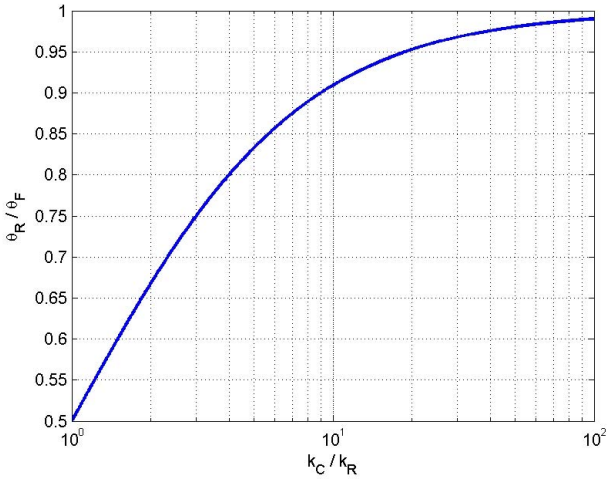

Figure 2. Static ratio of rear to front roll angle

Since the chassis compliance acts in series with the rear roll stiffness in Figure 1b, less of the rolling moment will be distributed to the rear axle than if the chassis did not warp. The rolling moment distribution observed on the rig compared to the ideal rolling moment distribution may be calculated using the relationship:

$$\frac{RMD}{RMD^*} = \frac{\left(\frac{k_C}{k_F + k_R}\right) + \left(\frac{k_R}{k_F + k_R}\right)}{\left(\frac{k_C}{k_F + k_R}\right) + \left(\frac{k_R}{k_F + k_R}\right)\left[1 - \left(\frac{k_R}{k_F + k_R}\right)\right]}, \tag{3}$$

where RMD and RMD* are the percentages of the roll moment distributed to the front axle for the compliant and rigid chassis models, respectively. This relationship is plotted in Figure 3. As this figure shows, the difference between compliant and rigid roll moment distribution decreases as the chassis stiffness increases relative to the total roll stiffness and the difference is worse as the roll stiffness distribution is biased towards the rear.

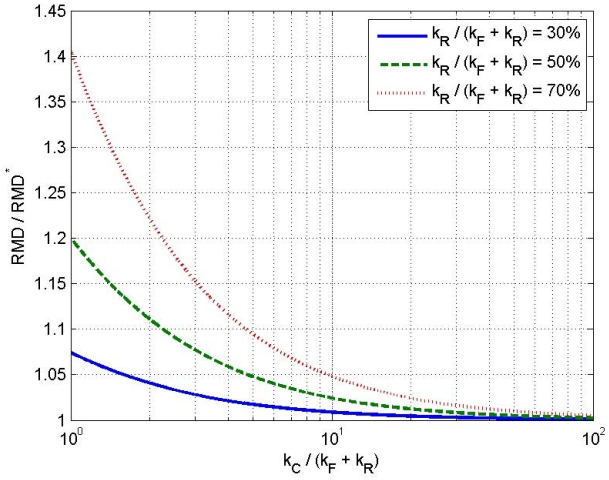

Figure 3. 7-post rig roll moment distribution compared to ideal moment distribution

In contrast to a 7-post shaker rig, an 8-post shaker rig can apply independent moments at both the front and the rear of the chassis, which allows the 8-post rig to achieve any desired front and rear roll angle within the safety limits of the vehicle and the rig.

EXPERIMENTAL SETUP

A series of tests were conducted using a NASCAR late model car on a Moog-FCS dynamic shaker rig at the Virginia Institute for Performance Engineering and Research (VIPER) facility, as shown in Figure 4.

Figure 4. NASCAR late model test vehicle on the rig

8-POST RIG - The VIPER 8-post shaker rig can be configured in either 7-post or 8-post mode, making it a unique test-bed for this analysis. Like a conventional 7-post rig, the tires are supported by four hydraulic actuators, or wheelloaders, that simulate displacement inputs from the track surface. Three or four pneumatic actuators, or aeroloaders, apply forces to the chassis to provide heave force, roll moment, pitch moment, and warp moment, which simulate the effect of inertial and aerodynamic forces present during a track test.

Figure 5. Left front wheelloader and aeroloader

Each tire is supported by a wheel platen, as shown in Figure 5. The wheel platen is mounted to the wheelloader, and provides the interface between the wheelloader and the tire. On the top of each wheel platen is a white Teflon plate, which reduces friction between the tire and the wheel platen. The force transmitted at the tire patch is measured by an array of load cells.

Each hydraulic wheelloader has a stroke of 14 inches, a control bandwidth of 100 Hz, can produce 7,400 lbs of dynamic force, and can achieve a peak velocity of 180 in/s. The wheelloaders are powered by a 200 HP, 100 GPM, 3000 psi hydraulic pump with over 30 gallons of accumulation to prevent transient pressure drops.

Either three or four pneumatic actuators, or aeroloaders, are also attached to mounts on the vehicle's frame using rod ends, as shown in Figures 5 and 6. Load cells mounted on each aeroloader shaft measure the static and dynamic applied force.

(a) (b)

Figure 6. Rear aeroloaders: (a) Left rear aeroloader in 8-post mode, (b) Rear aeroloader in 7-post mode

Each pneumatic aeroloader has a stroke of 24 inches, a control bandwidth of 10 Hz, can produce 4000 lbs of force, and achieve a peak velocity of 12 in/s. The aeroloaders are powered by a 50 HP air compressor,

which provides refrigerator-dried air at a working pressure of 120 psi.

The VIPER 8-post shaker rig is controlled by a Moog-FCS SmarTest real-time controller. The controller also includes 24 additional channels of analog data logging. Test management is performed using Moog-FCS's FasTest software on a PC networked to the controller. The software allows the user to define a sequence of instructions that define the actuator commands or drivefile, data acquisition, and safety limits.

TEST VEHICLE - The test vehicle used for the experimental comparison is a 2007 NASCAR Sprint Cup car. The suspension on this vehicle consists of an independent short-long arm (SLA) front suspension and a solid-axle trailing-arm rear suspension with Penske 7300 shock absorbers.

Only shock displacements and chassis ride height measurements were considered for the analysis in this paper. Each shock has a linear potentiometer mounted across it with a motion ratio close to unity. String potentiometers were mounted to the chassis to measure ride height. In 8-post mode, the aeroloaders were mounted to the chassis in the same locations that the laser ride height sensors were mounted. All sensors were calibrated and tared prior to the test such that all measured displacement data was recorded in inches.

EXPERIMENTAL TEST: TRACK DRIVEFILE

The first series of experimental tests compare the performance of a 7-post configuration with an 8-post configuration where the objective was to match the rig response to a particular target data file. This is a common task with all shaker rigs and requires the completion of a procedure known as *Drive File Identification*.

The target data file used for this test contained actual dynamic response measurements of the four shock displacements and four laser ride height measurements for one lap on a NASCAR-sanctioned track. Because they are not pertinent to the results of this paper, and in order to maintain confidentiality, details such as the track location, team name, the actual target data and information about lap times are intentionally omitted from this paper. It is actually more pertinent to present errors between the rig response and the target data.

Two separate drive files were developed for this test: one for the 8-post configuration and one for the 7-post configuration. In each case, every effort was made to ensure that the errors between the rig response and the common target data were as small as possible. After completing the drive file identification process, the final drive files were applied to the appropriate rig configuration and the final on-rig vehicle responses were recorded.

Figure 7 shows the resulting time history of the errors between the rig response and the target data over one lap. Four events have been identified in this time history to indicate times that are correlated to large deviations between 7-post and 8-post responses. Notice that the error in the 7-post response following these events tends to be significantly higher than for the 8-post response.

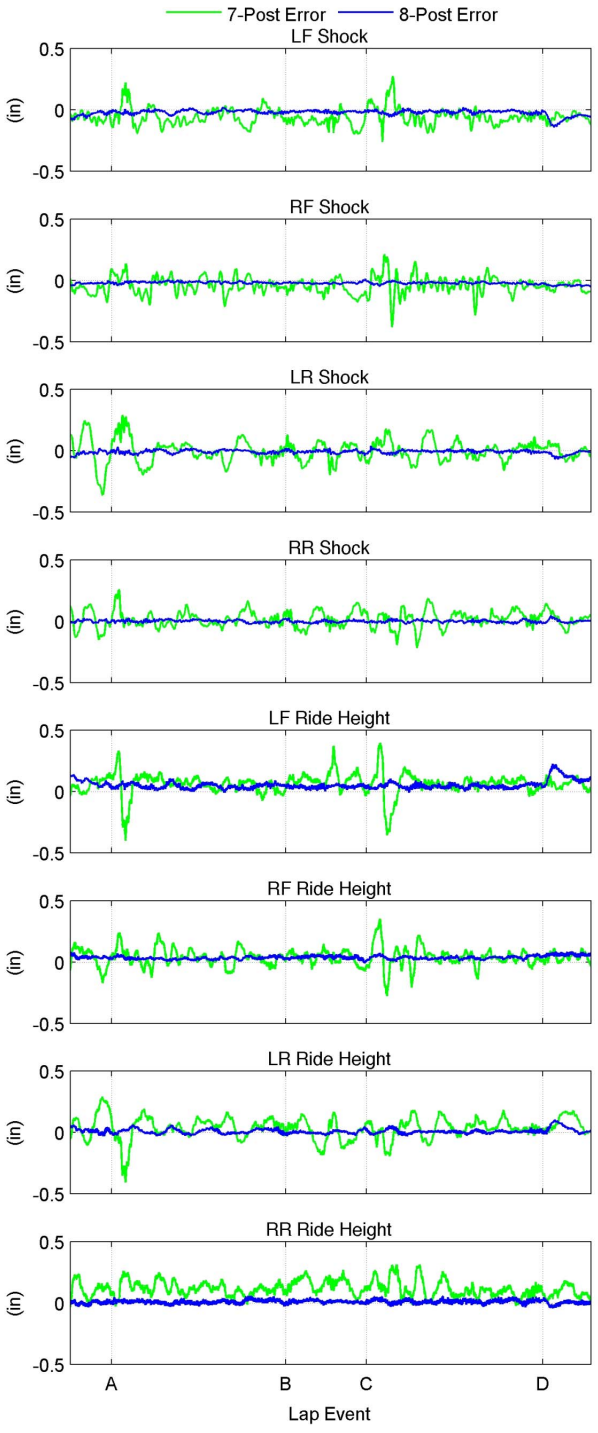

Figure 7. Experimentally achieved error between the target data and the actual responses

Using only the ride height measurement data, the chassis warp angle is computed and plotted in Figure 8 for the target data as well as for the 7-post and 8-post response data. Even though the drive file identification process did not explicitly attempt to minimize the warp error, Figure 8 indicates that the 8-post configuration matches the target warp angle fairly well.

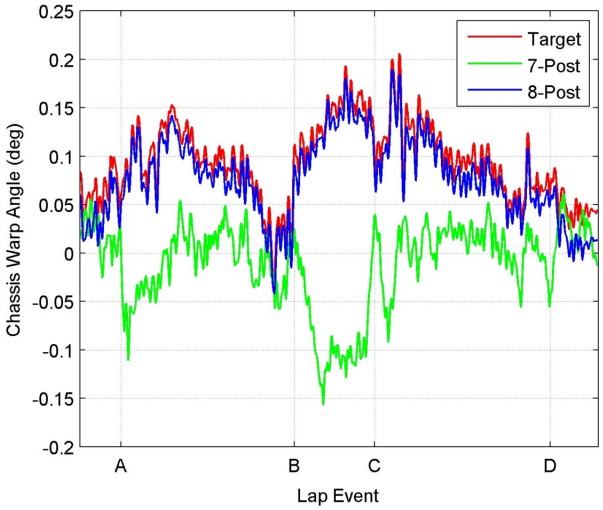

Figure 8. Experimentally achieved warp angles for 7-post and 8-post relative to the target data

Figure 8 also shows a clearer picture of the deviations between the 7-post response and the target response at the event markers. For example, at event B in Figure 8, the target warp is positive and increasing, but the 7-post configuration warp is negative and decreasing. The 7-post configuration is not able to generate the rear roll moment that is required to achieve the target warp angle. Also notice that during most of the lap, the target warp is positive where the 7-post warp is near zero with an occasional negative excursion.

EXPERIMENTAL TEST: ROLL WITH WARP

The second series of experimental tests also compared the performance of a 7-post with an 8-post configuration, but for this test, the target data was specifically designed to only consider roll and warp.

Figure 9 shows a plot of the target roll angles for the front and the rear as measured at the aeroloader attachment points. The desired rear roll angle was specified to be 10% larger than the front roll angle. This yielded a peak warp angle of 0.2 degrees, which matches the peak warp angle from the previous experimental results (see Figure 8). Based on the theoretical static model analysis above, the 7-post rig should not be able to achieve this condition. Also notice from Figure 9 that the warp angle is one-tenth of the nominal roll angle.

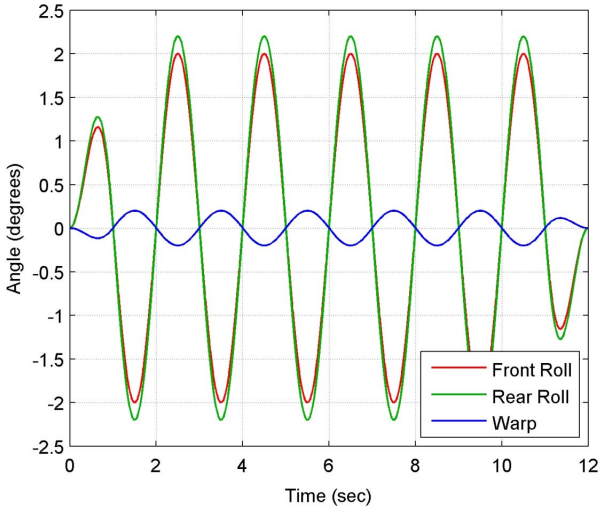

Figure 9. Desired roll angles are designed to induce warp with the rear roll greater than the front roll

The first two seconds of the target data in Figure 9 has a linear fade-in applied to it, and likewise the last two seconds of the data has a linear fade-out. The roll frequency was selected to be 0.5 Hz which essentially provides a quasi-static condition. The results below only show the steady response from 2 to 10 seconds.

As in the first experiment, two separate drive files were created using a formal drive file identification process for the 8-post and for the 7-post configurations. Again, every effort was made to ensure that the errors between the rig response and the target data were as small as possible. The target data for this experiment only used laser ride height measurements and aeroloader inputs. The wheel loaders were not used in this test other than to support the static load of the vehicle.

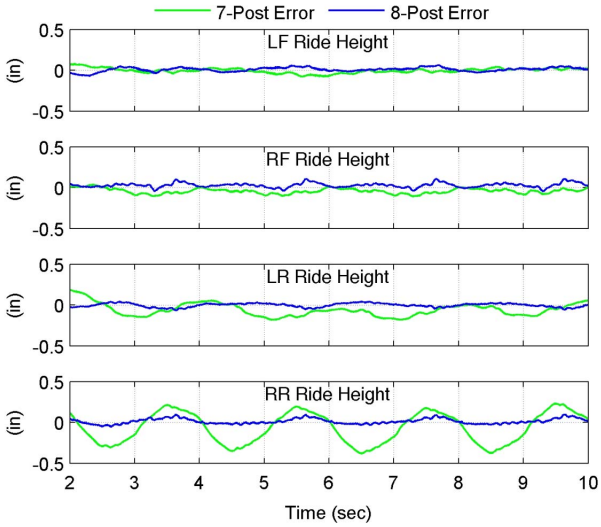

Figure 10. Experimentally achieved error between the target data and the actual ride heights

From the results in Figure 10, we see that the front ride height responses are very closely matching the target response for both 7-post and 8-post modes. Even the left rear (LR) ride height error is not too large, but the right rear (RR) ride height error for 7-post mode is unacceptable. Because there is only one aeroloader in the rear and because the front two aeroloaders are already matching the target response in the front, there is no way for the 7-post to reduce the error in the rear.

It is certainly possible in the drive file identification process to re-distribute the total error between all four sensors so that no one sensor has a large error; however, the 7-post configuration does not have enough degrees of freedom to match the target response so there will always be an error under such warp conditions.

The plots in Figure 11 use the exact same data as in Figure 10, but displayed as error between front, rear, and warp roll angle relative to the target for both the 7-post and the 8-post configurations. As expected, the front roll angle matches the target fairly well for both 7-post and 8-post, but there is a significant error in the rear roll angle and also the warp for the 7-post configuration. The error in the 7-post warp angle is as large as the target warp itself. This result is expected since the target data was designed with the rear roll angle larger than the front roll angle, but the theoretical static analysis indicates that the 7-post can only produce a static rear roll angle that is less than the front roll angle.

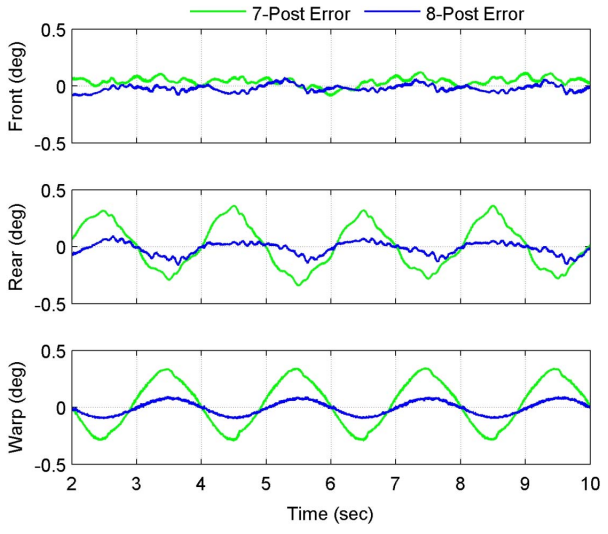

Figure 11. Experimentally achieved error between the target and the actual roll and warp signals

The peak residual error in the 8-post warp angle and rear roll angle is about the same amount as the peak residual error in the front roll angle.

SUMMARY

The simple static compliance model of chassis roll and warp indicated that a 7-post rig is perfectly adequate for vehicles with a rigid chassis. For a chassis that is not rigid, the ability of a 7-post shaker rig to match all target responses will necessarily be degraded. This result was experimentally confirmed on an actual late model NASCAR Sprint Cup car with two separate experiments. The first test used actual target data from a track test and the second test used fabricated target data designed to illustrate the limitations of 7-post testing. In both experiments, the 7-post rig was unable to match the performance of the 8-post shaker rig on all sensors.

ACKNOWLEDGEMENT

The authors wish to thank Petty Enterprises for their generous donation of the late model NASCAR Sprint Cup car which was used for this study.

REFERENCES

1. Bigliant U., Piccolo R., Vipiana C., “On Road Test vs Bench Simulation Test: a Way to Reduce Development Time and Increase Product Reliability,” SAE Paper No. 905207, 1990
2. Kelly, J.E., Kowalczyk, H., and Oral, H.A., “Track Simulation and Vehicle Characterization With 7 Post Testing,” SAE Motorsports Engineering Conference & Exhibition, December 2002, Indianapolis, IN, USA
3. Kowalczyk, H.R., “Damper Tuning with the Use of a Seven Post Shaker Rig,” *SAE 2002 World Congress & Exhibition*, March 2002, Detroit, MI, USA
4. Kasprzak, J.L., and Floyd, R.S., “Use of simulation to tune race car dampers,” SAE Technical Paper #942504, December 1994.
5. Thompson, L.L., Soni, P.H., Raju, S., and Law, E.H., “The effects of chassis flexibility on roll stiffness of a Winston Cup race car,” SAE Technical Paper 983051, 1998
6. Deakin, A., Crolla, D., Ramirez, J.P., and Hanley, R., “The effect of chassis stiffness on race car handling balance,” SAE Technical Paper, 2000-01-3554.